

1 **Magnetic immunochromatographic test for histamine detection in wine**

2 Amanda Moyano¹⁻², María Salvador^{2,5}, José C. Martínez-García², Vlad Socoliuc⁴, Ladislau Vékás⁴, Davi-
3 de Peddis⁵, Miguel A. Alvarez³, María Fernández³, Montserrat Rivas^{2*}, M. Carmen Blanco-López^{1*}

4

5 ¹Department of Physical and Analytical Chemistry, University of Oviedo, 33006 Oviedo, Spain

6 ²Department of Physics, University of Oviedo, 33204 Gijón, Spain

7 ³Dairy Research Institute of Asturias, IPLA (CSIC), Villaviciosa, Asturias, Spain

8 ⁴Laboratory of Magnetic Fluids, Center for Fundamental and Advanced Technical Research, Romanian
9 Academy - Timisoara Branch, 300223 Timisoara, Romania

10 ⁵Institute of Structure of Matter (CNR), 00015 Monterotondo Scalo (RM), Italy

11 *Corresponding authors: rivas@uniovi.es; cblanco@uniovi.es

12 **Abstract**

13 Histamine, a biogenic amine, is abundant in fermented foods and beverages, notably wine. A high in-
14 take of this monoamine may produce adverse reactions in humans, which may be severe in individuals
15 with a reduced capacity to catabolize extrinsic histamine. Thus, control of histamine concentration during
16 wine production and before distribution is advisable. Simple, rapid, point-of-use bioanalytical platforms
17 are needed because traditional methods for the detection and quantification of histamine are expensive
18 and time-consuming. This work applies the lateral flow immunoassay technique to histamine detection.
19 Superparamagnetic particle labels, and an inductive sensor designed to read the test line in the immunoas-
20 say, enable magnetic quantification of the molecule. The system is calibrated with histamine standards in
21 the interval of interest for wine production. A commercial optical strip reader is used for comparison
22 measurements. The lateral flow system has a limit of detection of 1.2 and 1.5 mg/L for the inductive and
23 optical readers, respectively. The capability of the inductive system for histamine quantification is
24 demonstrated for wine samples at different processing points (at the end of alcoholic fermentation, at the
25 end of malolactic fermentation, in freshly bottled wine, and in reserve wine). The results are validated by
26 ultra-high-performance liquid chromatography.

27 **Keywords:** biogenic amines; histamine; lateral flow immunoassay; superparamagnetic nanoparticles;
28 histamine biosensor.

29 1. Introduction

30 Biogenic amines (BAs) are basic nitrogenous compounds with low molecular weight and biological
31 activity. The most frequent among them are histamine, tyramine, tryptamine, putrescine and cadaverine,
32 and are present in several foodstuffs in a variable range of concentrations depending on the food (1). BAs
33 are produced by certain bacteria and yeasts during the fermentation of wines, and other beverages and
34 foods as beer, chocolate or cheese. They can also be produced by the normal metabolic activity of animal
35 and vegetal cells. However, in fermented products, where BAs can reach the highest concentrations, they
36 are normally generated by the microbial decarboxylation of the corresponding amino acids. In some cas-
37 es, these microorganisms, Gram-positive and Gram-negative bacteria, are part of the starter and/or the
38 secondary microbiota, necessary to produce the desired fermentation of the product. In other cases they
39 are present as food contaminants (2).

40 Histamine is one of the most abundant and toxic BAs in fermented foods. Even in small amounts it
41 can produce symptoms in susceptible individuals, and in high levels it can cause serious toxicological
42 problems (3). In alcoholic beverages, the toxic effects can be stronger due to the inhibition effect of alco-
43 hol on the intestinal epithelium detoxification system (4), which is one of the main reasons why it is so
44 important to analyse wines.

45 Despite the risk of histamine, there is no consensus in the legislation to regulate its concentration in
46 food. Only in fishery products the maximum histamine levels have been set at 50 mg/kg by the USA
47 Food and Drug Administration (5) and at 100 mg/kg by the European Community (6). In the case of
48 wine, there are no legal restrictions, but some European countries recommend upper limits that range
49 from 2 to 10 mg/L depending on the country (7-9). These considerations need to be taken into account to
50 facilitate commercial transactions.

51 But, besides the health risks of BAs, they can also affect the organoleptic quality of the wine. It has
52 been reported that histamine can be generated during different stages of the winemaking process: alcohol-
53 ic fermentation by yeasts (10, 11), malolactic fermentation by bacteria (12, 13) and ageing (14). Other
54 factors such as time, storage conditions (temperature and pH), raw material quality and the possibility of
55 contamination during aging can contribute to increase histamine content. All kind of wines may contain
56 BAs, but typically red wines have more than other varieties (white, rose, rice and Porto) due to their vi-
57 nification processes (15), and even high-rated wines may have them.

58 These considerations have prompted attentive wine producers and consumers to get interested in bio-
59 analytical methods that are fast and unsophisticated to detect and quantify BAs for sensitive individuals
60 and wine producers both during the winery process and in the final product.

61 Up to now, different methods have been reported to detect BAs. Currently, the most used analytical
62 technique is Liquid Chromatography (LC) coupled to ultraviolet, fluorescence or mass spectrophotometry
63 detectors (16). Gas Chromatography (GC) is a faster alternative for which pre-derivatization is required to
64 increase the volatility and decrease polarities of the BAs (17). Capillary Electrophoresis (CE) is the sec-
65 ond most common technique for BAs determination because is very adequate for screenings (18). The
66 chromatographical techniques described above (LC, GC and CE) give a precise and sensitive analysis of
67 numerous BAs simultaneously. However, they are time consuming, require expensive instruments and
68 qualified personnel. Non-chromatographic analyses are alternatives that include biosensors (19-21), En-
69 zyme Linked Immunosorbent assay (ELISA) (22), and flow-injection analysis (23). These methods are
70 faster but require sample pre-treatment to clean up matrix interferences. Moreover, they still require spe-

71 cialized personnel and are difficult to implement in a cellar, where a rapid respond with the minimum
72 complexity is needed.

73 Lateral Flow Immunoassay (LFIA) is a powerful point-of-use system for simple, rapid, portable and
74 low-cost analysis in different fields (clinical diagnosis, food safety and environment). The LFIA tech-
75 nique is based on an immunochromatografic separation at nitrocellulose dipsticks, as sample flows by
76 capillary action. The test involves different cellulosic materials (sample pad, conjugate pad, nitrocellulose
77 membrane and adsorption pad) assembled on a plastic backing to get robustness. The recognition of the
78 analyte relies on the use of specific molecules immobilized on the membrane in two lines (test and control
79 lines). LFIA combines the technology of ELISA and chromatography, overcoming some drawbacks of
80 both methods, such as time-consumption and complexity. There are different formats depending on the
81 analyte. The most common are: sandwich format, in which two antibodies are used to recognize the ana-
82 lyte, and competitive format for low molecular weight compounds, such as histamine, in which a single
83 antibody is available for the recognition of the molecule of interest. Several systems have been used as
84 reporter labels in LFIAs: gold, iron oxide, carbon, selenium or silver nanoparticles (NPs), coloured latex
85 beads, quantum dots, enzymes or liposomes. Frequently, LFIA operates on a purely qualitative basis,
86 displaying a positive/negative answer. Motivated by the concern on fishery products, lateral flow devices
87 for a rapid visual detection of histamine have been developed (24), some of which can be applied also to
88 wine. These tests are aimed at detecting unsafe levels of histamine according to legal regulation on fish,
89 so they provide a positive/negative response with a threshold of 50 ppm or 200 ppm.

90 This article focuses on adding quantitative capacities to LFIAs for histamine in red wine, while re-
91 ducing the LOD to levels to match the European recommendations for this product (2-10 ppm). Associat-
92 ing the LFIA to a reading equipment which does not compromise the rapidity and simplicity of the test is
93 major challenge (25). Recently, magnetic nanoparticles have been proposed as LFIA labels to enable,
94 besides the visual detection, magnetic quantification (26-29). The authors have reported on a novel induc-
95 tive sensor to quantify superparamagnetic particles without the application of exciting fields, which large-
96 ly reduces the complexity and cost of the device (30, 31). The system, adapted for LFIA strips has been
97 successfully used to determine prostate specific antigen concentrations in the clinical range of interest by
98 using a sandwich format (32). This measuring device does not require bulky components. This means that
99 it can be easily miniaturised to a point-of-use portable device.

100 In this article we use this novel approach to detect and quantify histamine, in the concentration range
101 of interest for wines. Although the thresholds already adopted as recommendation in some EU countries
102 are 2–10 mg/L, studies on 100 selected high-quality red wines made from seven different cultivars found
103 that 34% were above this limit and as high as 27 mg/L (9). The range of interest widens then to 1–100
104 mg/L.

105 We report for the first time on a histamine quantification technique for red wine based on a magnetic
106 competitive LFIA. Red wine is especially challenging to its intensely coloured matrix, that implies high
107 background and poor reliability for the traditional optical readers. The purple colour of red wine aggra-
108 vates the problem as the classical labels are gold NPs that yield a similar red-purple colour. Therefore,
109 this work was aimed at developing a LFIA based on superparamagnetic labels. The immunoassay is com-
110 bined to an inductive sensor capable to quantify the magnetic moment of such labels. The system has
111 been tested with red wine samples and validated against Ultra High-Performance Liquid Chromatography
112 (UHPLC) analyses. The system proved to be successful as histamine point-of-use analytical technique in
113 the range of regulatory concern.

114 2. Materials and methods

115 2.1 Reagents and instruments for the immunoassay

116 Mouse histamine monoclonal antibody (MBS2025715) and histamine-BSA conjugate antigen
117 (MBS358205) were purchased from Mybiosource. Anti-mouse IgG, Bovine Serum Albumin (BSA), 1-
118 ethyl-3-[3-dimethylaminopropyl]-carbodiimide hydrochloride (EDC), N-hydroxysuccinimide (NHS), 2-
119 (N-Morpholino)ethanesulfonic acid (MES) and histamine dihydrochloride were provided by Sigma-
120 Aldrich (Spain). Recombinant protein A/G was purchased at Thermo-Scientific (Massachusetts, USA).
121 Gold nanoparticles of size 40 nm were purchased from BB International (UK). Disposable 0.45 μm
122 PVDF filters were purchased from GE Healthcare Life Sciences.

123 Glass fibre membrane (GF001000) used as sample pad and backing cards (HF000MC100) were
124 purchased from Millipore (Germany). Other materials used were nitrocellulose membranes (UniSart
125 CN95, Sartorius, Spain) and absorbent pads (Whatman, USA). Based on previous results, the sample
126 buffer consisted of 10 mM Phosphate-Buffer (PB) pH 7.4 with 0.5% Tween-20 and 1% BSA.

127 An IsoFlow reagent dispensing system (Imagene Technology, USA) was used to dispense the detec-
128 tion lines (dispense rate 0.100 $\mu\text{L}/\text{mm}$) and the strips were cut with a guillotine Fellowes Gamma (Spain).
129 A portable strip reader ESE Quant LR3 lateral flow system (Qiagen Inc., Germany) was used to quantify
130 the intensity of the test line by reflectance measurements.

131 2.2 Functionalization of labels with protein A/G

132 Protein A/G was conjugated to gold nanoparticles for its functionalization. A gold colloidal titration
133 was carried out to find the optimal concentration of protein A/G to stabilize the gold nanoparticles. The
134 titration experiments show that 1.5 mg/mL of protein is the optimal concentration for its functionaliza-
135 tion. For the conjugation, 100 μL of 1.5 mg/mL protein A/G was added to 1.5 mL of gold nanoparticles in
136 suspension. After shaking for 1 h, 100 μL of blocking solution (1 mg/mL BSA in PB 10 mM, pH 7.4) was
137 added to block the residual surfaces of the gold conjugate. After 20 min of blocking reaction, the mixture
138 was centrifuged at 6,800 g for 20 min. The supernatant was discarded, and the pellet was resuspended in
139 2 mM of PB buffer, pH 7.4, with 10% sucrose and 1% BSA. The conjugates protein A/G-gold nanoparti-
140 cles were stored at 4 $^{\circ}\text{C}$ until used.

141 Superparamagnetic magnetite nanoparticles prepared by a coprecipitation route and coated with a
142 double layer of oleic acid (33) were functionalized using recombinant protein A/G to develop the immu-
143 noassay. Firstly, the carboxyl groups of the nanoparticles were activated using the carbodiimide chemis-
144 try. For this, 100 μL of EDC (5 mg/mL in MES 50 mM, pH 6.00), 100 μL of NHS (5 mg/mL in MES
145 50 mM, pH 6.00) and 100 μL of recombinant protein A/G (different concentrations were used to optimize
146 the assay) were mixed with 10 μL of nanoparticles. After shaking for 4 h, the residual carboxyl groups on
147 the surfaces were blocked by adding 100 μL of the blocking solution (1% BSA in PB 10 mM, pH 7.4).
148 Then, the mixture was centrifuged at 21,448 g for 20 min. Finally, 300 μL of supernatant was discarded
149 and the pellet was resuspended in PB 10 mM, pH 7.4.

150 2.3 Characterization of nanoparticles conjugates by Dynamic Light Scattering

151 Size distribution and ζ -potential assays were carried out with a Zetasizer Nano ZS ZEN3600 (Mal-
152 vern Instruments, Malvern, UK) equipped with a solid-state He-Ne laser (633 nm). This instrument was

153 used to monitor the conjugation process. A total of three readings were carried out at 25 °C. Each reading
154 was composed of 15 measurements of the backscattered (173 °) intensity. Zetasizer software version 7.03
155 was used for data processing and analysis.

156 2.4 Preparation of the immuno-strips

157 The competitive LFIA to detect histamine was carried out in a dipstick format. The nitrocellulose
158 membrane (25 mm-wide) was incorporated into a backing plastic card to make it robust enough. Two
159 lines of antibodies were immobilised across the nitrocellulose strip: (i) the test line to provide the result of
160 the analysis, and (ii) the control line to get the guarantee that the liquid sample has flowed adequately
161 along the strip. Both lines were applied by the IsoFlow dispenser at a rate of 0.100 $\mu\text{L}/\text{mm}$. A 1 mg/mL
162 concentration of histamine-BSA conjugate was used for the test line and a 1 mg/mL concentration of anti
163 IgG for the control line. The nitrocellulose membrane was dried for 20 min at 37 °C after the immobiliza-
164 tion of the control and test lines. Then, the sample pad and the absorbent pad were settled onto a backing
165 card with an overlap between them of 2 mm. The complete strip was cut into individual 5 mm wide dip-
166 sticks.

167 2.5 Magnetic quantification

168 To provide a quantitative signal of the test line an inductive sensor specially developed for strip im-
169 munoassays was used (32). Its sensing head consists of a double copper line printed on a rigid insulating
170 substrate across which alternating current flows. The magnitude and phase of the sensing head impedance
171 are continuously monitored by a precision impedance analyser (Agilent 4294A) using 16048G test leads
172 and 500 mV/20 MHz excitation voltage. The change of magnetic permeability produced by the particles
173 in the surrounding of the conductor increases significantly its impedance. The test lines on the strips were
174 scanned laterally over the sensing head by a micro-positioner, producing a peak of the impedance signal
175 over the base line that is integrated to account for all the particles in the line no matter how they are dis-
176 tributed. The signal provided by the sensor is then measured in $\Omega \cdot \text{mm}$ coming from the cumulative inte-
177 gral of the impedance (Ω) across the width of the test line (mm). This alteration in the impedance is di-
178 rectly proportional to the number of superparamagnetic nanoparticles at the test line. As the magnetic NPs
179 were used in the strips as labels, this approach was used to calibrate the quantification of histamine. After
180 the calibration with histamine standards, a similar procedure was used to quantify the concentration of
181 histamine in real red wine samples.

182 2.6 Optical measurements

183 A portable strip reader ESE-Quant LR3 lateral flow system (Qiagen Inc., Germany) was used to
184 quantify the colour intensity of the test line by reflectance measurements. The optical reader analyses the
185 reflectance at the control and test line by using two channels (LED excitation and photodiode detection).
186 The reader scans the strip by illuminating it with a light beam and then measures the attenuation from the
187 surface of the strip through a confocal detector. The detector registers the signal and converts it into an
188 electrical signal that is related to the amount of analyte at the control and test lines. The device provides
189 values in units of $\text{mm} \cdot \text{mV}$, resulting from integrating the electrical signal (mV) across the width of the
190 test line (mm).

191 2.7 Validation by Ultra High-Performance Liquid Chromatography (UHPLC) meas- 192 urements

193 The wine samples were prepared and analysed by UHPLC following a method reported elsewhere
194 (34). The samples analysed correspond to red wine from different elaboration stages, at the end of the
195 alcoholic fermentation (sample A), freshly bottled (sample B), reserve wine (sample C) and at the end of
196 the malolactic fermentation (samples D and E), all from the Vino de Cangas Protected Origin Region
197 (from Asturias in Spain).

198 3. Results and discussion

199 3.1 Optimization of the immunoassay

200 The first step to develop the immunoassay was to optimize the amount of protein used to coat the na-
201 noparticles and the concentration of antibody.

202 3.1.1 Protein A/G concentration for nanoparticles conjugation

203 Different concentrations of recombinant protein A/G were tested (1, 2 and 3 mg/mL). Dynamic Light
204 Scattering (DLS) measurements were carried out to confirm the conjugation reaction. This technique
205 allows comparison between nanoparticles hydrodynamic size before and after the conjugation reaction.
206 The hydrodynamic diameter of nanoparticles before conjugation was 86.6 nm (PDI 0.2). The ζ -average of
207 the hydrodynamic sizes were 479.8 nm (PDI 0.4), 193.0 nm (PDI 0.4) and 120.8 nm (PDI 0.3) after con-
208 jugation with 1 mg/mL, 2 mg/mL and 3 mg/mL of protein, respectively (Figure 1). The results showed
209 that, for all concentrations of protein A/G, the nanoparticles size increased after the addition of the pro-
210 tein. This demonstrates that the conjugation process through the carbodiimide chemistry was successful.
211 Furthermore, the diameter of the conjugates was larger when concentration of the protein was lower. This
212 could be explained because a protein molecule could bind to several nanoparticles when there were not
213 enough molecules to cover every single nanoparticle, thus aggregates were formed.

214 

215 **Figure 1** Hydrodynamic size distribution profiles of superparamagnetic iron oxide nanoparticles before
216 (solid black line) and after conjugation with concentrations of 1 mg/mL (red), 2 mg/mL (blue) and 3 mg/mL
217 (dashed) of protein A/G.

218 With the aim to select the most suitable protein concentration, the immunoassay without histamine
219 (blank sample) was carried out in the range 1–3 mg/mL and the line tests were analysed by reflectance
220 measurements using reader ESE-Quant LR3 lateral flow system. In all cases, the aggregates were able to
221 flow through the nitrocellulose membrane by capillarity. The results of the measurements of the test line
222 yielded values of 909.99, 845.73 and 639.40 mm·mV for 1 mg/mL, 2 mg/mL and 3 mg/mL of protein,
223 respectively. The reflectance signal increases when the diameter of protein A/G-NP conjugates is larger
224 because in this case there are more NPs attached to each antibody unit. These agglomerates have a signal
225 amplification effect, proportional to the size of the conjugate. In view of these results we concluded that
226 1 mg/mL of recombinant protein A/G produced the largest signal. Therefore, this was the concentration
227 chosen for the next experiments.

228 3.1.2 Anti-histamine antibody concentration

229 Different concentrations of antibody were assayed in order to optimise the signal. This step was made
230 with gold conjugates and used to estimate the antibody concentration for the competitive assay. The anti-
231 body was added during the first step of the immunoassay and therefore, direct binding to the histamine-
232 BSA complex immobilized on the membrane occurs. For the immunoassays 13, 10, 9 and 5 mg/L of
233 antibody were used. The reflectance measurements yielded 996.97, 984.62, 862.05 and 431.48 mm-mV,
234 respectively. Finally, 10 mg/L was chosen because, even when the signal increases with the concentra-
235 tion, there were not significant differences between 10 and 13 mg/L.

236 3.2 Competitive lateral flow immunoassay procedure

237 The test to quantify histamine is based on a competitive immunoassay, thus the relationship between
238 the concentration and signals, either magnetic or optical, tends asymptotically to zero. The procedure
239 consists of two steps, as illustrated in **Error! No se encuentra el origen de la referencia.** The first step
240 is the competition of the anti-histamine antibodies in solution for the histamine in the sample and the one
241 immobilized at the test line. The second step is the colour developing, based on the retention of the con-
242 jugate protein A/G-NP at the test line thanks to the ability of protein A/G to bind to antibodies of any
243 kind. The surplus of protein A/G-NP (not retained at the test line) proceed along the strip and are trapped
244 at the control line by the Fc region of the anti-IgG and anti-histamine antibodies (see Figure 2).

245 In order to calibrate the strips, several histamine standard solutions were prepared in 10 mM PB and
246 pH 7.4. The competitive LFIA was carried out in dipstick format. For the first step, 10 μ L of histamine of
247 different concentrations and 2 μ L of anti-histamine antibody (0.5 mg/mL) were transferred into a micro-
248 tube from a stock solution to get a final concentration of the anti-histamine antibody of 10 mg/L. Then
249 buffer was added always keeping a final volume of 100 μ L (98 μ L of buffer for the blank and 88 μ L of
250 buffer for the samples). The optimized running buffer had 1% BSA. The sample pad was introduced into
251 the mixture and the solution flowed along the strip by capillary action. After 30 min, 10 μ L of NPs coated
252 with protein A/G and 90 μ L of running buffer were added to the microtube for the developing step.

253 

254 **Figure 2** Schematic illustration of the competitive LFIA. (A) First step: immobilization of the anti-
255 histamine antibodies. (B) Second step: colour development.

256 3.3 Histamine standards calibration

257 To calibrate the strips, several histamine standard solutions were prepared by dilution and assayed
258 following the procedure previously described. In a first run the experiments were conducted in a wide
259 range of histamine concentrations. The protein concentration in the functionalization protocol was 1.5 and
260 2 mg/mL for gold and magnetic nanoparticles respectively. Figure 3 shows the calibration curves in the
261 immunoassays using gold (red) and iron oxide (black) NPs as labels. Six standard samples with histamine
262 concentrations in the range from 10^{-3} to 10^2 mg/L, besides a negative reference sample, were run by trip-
263 licate and measured with the optical reader. The results yield sigmoid-shape profiles, characteristic of
264 competitive immunoassays. For very low concentrations, the curve has an asymptotic behaviour as a
265 result of the total occupancy of the immobilized histamine-BSA complexes by anti-histamine antibodies.
266 The measured points have been fitted in Figure 3 (dotted lines) using the four-parameter logistic equation:

$$S = \frac{\alpha - \delta}{1 + (C/\gamma)^\beta} + \delta \quad (1)$$

267 where S and C are the sensor measurement and the histamine concentration, α and δ are the S -values of
 268 the upper and lower asymptote, respectively, β is the slope at the inflection point, and γ is the value of C
 269 corresponding to 50% of the maximum asymptote (35). The parameters values used for the fits of Fig-
 270 ure 3 were respectively $\alpha = 1110$ mm·mV, $\beta = 0.8$, $\gamma = 5.3$ mg/L and $\delta = 160$ mm·mV (red line) and
 271 $\alpha = 1130$ mm·mV, $\beta = 0.8$, $\gamma = 4.5$ mg/L and $\delta = 190$ mm·mV (black line). This first analysis leads to
 272 the conclusion that quantification is feasible in the range of 1–100 mg/L for the gold nanoparticles and
 273 0.1–100 mg/L for the iron oxide superparamagnetic particles. Besides their wider working range, iron
 274 oxide NPs have the advantage of enabling the magnetic pre-concentration of the analyte. Although this
 275 procedure has not been yet tested in histamine immunoassays, it has been commonly used for pre-
 276 concentration of analytes associated to different bioanalytical techniques (36). This allows bringing the
 277 samples with lower concentrations into the working range by a simple magnetic pre-treatment.

278 Insert Figure 3

279

280 **Figure 3** Quantification of LFIA by the optical reader using gold (red) and iron oxide (black) NPs. The
 281 lines plotted to guide the eye are four-parameter sigmoid curves. Inset: One of the series of standard sam-
 282 ples used to obtain the red curve, with the control line on top and the test line below.

283

284 Figure 4 shows a detailed calibration with magnetic NPs in the range 1–100 mg/L. For this, the A/G
 285 protein concentration for functionalization was optimized according to the DLS results. Optical and in-
 286 ductive readers have been used, the latter yielding better correlation factor. Dotted lines represent the
 287 least-squares linear fit of the data; slopes, y -intercepts and correlation factors are also shown on the graph.
 288 The limits of detection (LOD) have been calculated following ref. (37) from the blank-subtracted results
 289 and gives values of 1.2 mg/L and 1.5 mg/L for the inductive and optical methods, respectively.

290

291 Insert Figure 4

292 **Figure 4** Inductive (left axis) and optical (right axis) signals of the magnetic LFIA as a function of the con-
 293 centration of histamine. Least-squares linear regression curves are plotted as dotted lines. Inset: One of the
 294 series of standard samples used to obtain the plotted lines. The control line is on top and the test line below.

295 3.4 Application to wine samples

296 The analytical method was tested against five samples of red wine taken at different stages of the fab-
 297 rication. The only pre-treatment was a simple filtering through a 0.45 μm PVDF filter. All the assays
 298 were performed in triplicate. The strips were measured with the inductive reader once dried, to get a
 299 quantitative reproducible reading.

300 Initial tests were done with both type of particles, iron oxide and the traditional colloidal gold. For
 301 comparison, Figure 5 shows an image of both types of strips after running a sample of red wine. Even a
 302 naked eye inspection allows concluding that red wine stains the white paper. This is especially remarka-
 303 ble in the case of gold labels which seem not to flow as well as magnetite. In such case, a quantitative
 304 determination by optical measurements becomes impossible or is very poor. For this reason, together with

305 the better results yielded by the calibration, the combination of iron oxide NPs and inductive sensor was
 306 chosen to perform the histamine quantification. The results are summarized in Table 1.

307 Insert Figure 5

308 **Figure 5** LFIA run with red wine samples using (A) superparamagnetic nanoparticles and (B) colloidal
 309 gold as reporters.

310 To validate the results, wines were also analysed by UHPLC and the results of histamine content are
 311 compared in Table 1. The error in the UHPLC measurements comes from the injection volume, which has
 312 been considered the only significant source of error. In the case of the LFIA, several error sources were
 313 identified that influence the inductive signal value: the printing of the antibody across the membrane
 314 (which may have small inhomogeneities in the line width), the guillotine cut of the strip from the mem-
 315 brane original card (this produces variability in the width of the strips), and the sensor resolution. Consid-
 316 ering that the errors produced are probabilistically independent, we can use the rule of error propagation
 317 to add up the relative errors. For this calculation three strips have been run with each wine and each of
 318 them has been measured four times. The resulting uncertainty of the sensor signals for the different wines
 319 is in the range 2–18% for the optical measurement and 2–5% for the inductive sensor. The uncertainties
 320 of the concentrations shown in Table 1 have been obtained by the propagation rule applied to the calibra-
 321 tion curve considering the errors of the slope and y-intercept given in Figure 4.

322 The LFIA values of the histamine content measured with the commercial optical reader are deficient.
 323 Moreover, the relative uncertainties are unacceptable due mainly to a considerable variability in the three
 324 strips of each wine. The problem is associated to the variability in colour intensity of the three strips of
 325 each wine more than a lack of sensitivity of the reader itself. For this method to be useful for quantifica-
 326 tion, the removal of the interfering matrix would be necessary. In contrast, the LFIA histamine levels
 327 given by the inductive reader are remarkably similar to the reference, taking into account the margins of
 328 error. Only wines D and E fall out of these ranges, the average LFIA value being overestimated in about a
 329 30%.

330 To investigate the possible origin of this deviation, several BAs have been quantified by UHPLC in
 331 the wines under study, namely, histamine, putrescine, cadaverine, tyramine, phenylethylamine and trypt-
 332 amine (see Table 2).



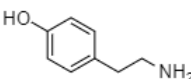
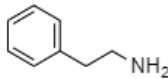
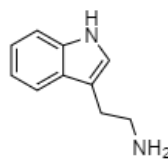
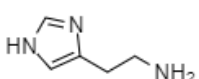
333 **Table 1** Results obtained by magnetic LFIA coupled to the inductive sensor and UHPLC for the red wine
 334 samples analysed in this work.

Wine	Stage of fabrication	LFIA & inductive sensor		LFIA & optical sensor		UHPLC	
		mg/L	mM	mg/L	mM	mg/L	mM
A	End of the alcoholic fermentation	46 ± 2	0.41 ± 0.02	25 ± 3	0.22 ± 0.03	44 ± 3	0.39 ± 0.03
B	Freshly bottled	82 ± 4	0.74 ± 0.04	56 ± 14	0.50 ± 0.13	83 ± 3	0.74 ± 0.03
C	Reserve wine	25 ± 3	0.22 ± 0.03	10 ± 1	0.09 ± 0.01	20 ± 3	0.18 ± 0.03
D	End of the malolactic fermentation	63 ± 4	0.57 ± 0.04	37 ± 7	0.33 ± 0.06	46 ± 3	0.42 ± 0.03
E	End of the malolactic fermentation	65 ± 5	0.58 ± 0.05	101 ± 18	0.90 ± 0.16	55 ± 3	0.49 ± 0.03

335

336
337

Table 2 Concentrations of biogenic amines by UHPLC. All the samples are red wine at different steps of the fabrication.

Biogenic amines	Structure	Wine A (mM)	Wine B (mM)	Wine C (mM)	Wine D (mM)	Wine E (mM)
Putrescine		1.717	1.842	0.754	1.417	1.769
Cadaverine		0.025	0.050	0.049	0.063	0.060
Tyramine		0.108	0.375	0	0.406	0.623
Phenylethylamine		0.072	0.418	0.452	0.112	0.350
Tryptamine		0	0	0	0	0
Histamine		0.39	0.742	0.175	0.416	0.494

338 Of all the amines analysed, tyramine has a similar structure to histamine, and reaches higher values in
 339 wines D and E, so it is likely to be producing a cross-reaction effect. In order to test this hypothesis, we
 340 have run the test with standard solutions of histamine (H) and tyramine (T). In one case, we have used 2.5
 341 µg of histamine while in the other we have also added 6.5 µg of tyramine. This leads to tests with 0.22
 342 and 0.69 mM concentration of BAs. These tests were performed with iron oxide NPs as labels and evalu-
 343 ated with the inductive sensor. The results are shown in Table 3 together with the “apparent histamine
 344 amount,” that is obtained applying the calibration parameters given in Figure (4). It can be concluded that
 345 the presence of tyramine interferes at the test, which displays lower magnetic signals and give rise to a
 346 value of histamine 27% larger than the nominal one. Another parameter that can be affecting these results
 347 is the different flowing velocity of the samples due to the matrix composition and viscosity. Although
 348 further research is needed to improve the reliability of the test, the results of LFIA are a proof of the ca-
 349 pability of the system not only to detect, but also to quantify histamine in red wine in the range of interest
 350 for wineries and sensitive consumers.

351 **Table 3** Cross reactivity study. The letters H and T stand for histamine and tyramine, respectively.

BAs	Concentration of BAs (mM)	Signal by inductive measurements (mm·mV)	Apparent concentration of histamine (mg/L) / (mM)
H	0.22	1.5	26 / 0.23
H + T	0.69	1.3	33 / 0.28

352

353 4. Conclusions

354 A biosensor for histamine quantification in red wines has been developed based on the combination
355 of magnetic competitive lateral flow immunoassay strips and an inductive sensor to perform the reading
356 out. The labels are superparamagnetic iron oxide nanoparticles 10 nm in size with a double lipidic layer
357 as coating that enables their functionalization. The magnetic perturbation of the NPs is detected by the
358 inductive sensor as an increase of its impedance proportional to the number of NPs in the test line, which
359 is in turn proportional to the number of anti-histamine antibodies. The system has been calibrated with
360 histamine standard solutions. To validate the new method, the competitive immunoassay has been done
361 also with traditional gold NPs and evaluated, both with gold and magnetite, with a commercial reflectance
362 reader. The combination of magnetic particles and inductive reader gave the best calibration correlation
363 factor and LOD, besides the well-known magnetic pre-concentration potential.

364 Finally, the system was tested for reliability and validity with five real red wine samples correspond-
365 ing to different stages during vinification and the final consumption state. In this case, the magnetic parti-
366 cles proved a new advantage compared to colloidal gold, which is a better flow of the wine sample along
367 the paper resulting in a cleaner strip. In addition, the magnetic inductive signal does not depend on the
368 dyeing of the paper, which is a complication for gold labels whose reading relies on an optical signal.

369 The measurements were cross-checked by UHPLC, leading to the finding that in two of the wine
370 samples they can be overestimated in about 30%, probably due to cross reactivity with tyramine. Despite
371 this, the conclusion is that the analytical method based on magnetic LFIA is very promising for point-of-
372 use determination of histamine. Keeping the advantages of simplicity, rapidity and low cost of traditional
373 LFIA, the magnetic character of the labels and their detection principle provide additional advantages like
374 the avoidance of sample pre-treatment for matrix removal, possibility of magnetic pre-concentration for
375 low concentration samples, improved calibration and LOD.

376

377 5. Acknowledgements

378 Wine samples were kindly provided by Juan M. Redondo from DOP Vino de Cangas. The authors
379 acknowledge the technical assistance of Begoña Redruello (IPLA) in the chromatographic analysis in
380 wine samples. This work was supported by the Spanish Ministry of Economy and Competitiveness under
381 projects MAT2017-84959-C2-1-R, MAT2016-81955-REDT and AGL2016-78708-R, the Council of
382 Gijón-IUTA under grant SV-18-GIJON-1-27, and the Principality of Asturias under project
383 IDI/2018/000185.

384 6. Conflict of interest

385 The authors declare no conflict of interest.

386 7. References

387 1. Ordóñez JL, Troncoso AM, García-Parrilla MDC, Callejón RM. Recent trends in the determination
388 of biogenic amines in fermented beverages – A review. *Analytica Chimica Acta*. 2016;939:10-25.

- 389 2. Daniel ML, MaCruz M, Victor L, Miguel AA, María F. Biogenic Amines in Dairy Products. *Critical*
390 *Reviews in Food Science and Nutrition*.51(7):691-703.
- 391 3. Ladero V, Calles-Enriquez M, Fernandez M, A. Alvarez M. Toxicological Effects of Dietary
392 Biogenic Amines. *Current Nutrition & Food Science*. 2010;6(2):145-56.
- 393 4. Bodmer S, Imark C, Kneubühl M. Biogenic amines in foods: Histamine and food processing.
394 *Inflammation Research*. 1999;48(6):296-300.
- 395 5. FDA. Fish and Fishery Products Hazards and Controls Guidance, Fourth Edition, Chapter 7. April
396 2011;113.
- 397 6. EU Directive, Regulation (EC) No 1441/2007 of 5 December 2007. *Official Journal of European*
398 *Union*. 2007.
- 399 7. Bauza T, Blaise A, Daumas F, Cabanis JC. Determination of biogenic amines and their precursor
400 amino acids in wines of the Vallée du Rhône by high-performance liquid chromatography with
401 precolumn derivatization and fluorimetric detection. *Journal of Chromatography A*. 1995;707(2):373-9.
- 402 8. Landete JM, Ferrer S, Polo L, Pardo I. Biogenic Amines in Wines from Three Spanish Regions.
403 *Journal of Agricultural and Food Chemistry*. 2005;53(4):1119-24.
- 404 9. Konakovsky V, Focke M, Hoffmann-Sommergruber K, Schmid R, Scheiner O, Moser P, et al.
405 Levels of histamine and other biogenic amines in high-quality red wines. *Food Additives &*
406 *Contaminants: Part A*. 2011;28(4):408-16.
- 407 10. Caruso M, Fiore C, Contursi M, Salzano G, Paparella A, Romano P. Formation of biogenic amines
408 as criteria for the selection of wine yeasts. *World Journal of Microbiology and Biotechnology*.
409 2002;18(2):159-63.
- 410 11. Goñi DT, Azpilicueta CA. Influence of Yeast Strain on Biogenic Amines Content in Wines:
411 Relationship with the Utilization of Amino Acids during Fermentation. *American Journal of Enology and*
412 *Viticulture*. 2001;52(3):185-90.
- 413 12. Lonvaud-Funel A. Biogenic amines in wines: role of lactic acid bacteria. *FEMS Microbiology*
414 *Letters*. 2001;199(1):9-13.
- 415 13. Iranzo JM, Ferrer S, Pardo I. Which lactic acid bacteria are responsible for histamine production in
416 wine? *J Appl Microbiol*2005. 580-6 p.
- 417 14. Hernández-Orte P, Lapeña AC, Peña-Gallego A, Astrain J, Baron C, Pardo I, et al. Biogenic amine
418 determination in wine fermented in oak barrels: Factors affecting formation. *Food Research International*.
419 2008;41(7):697-706.
- 420 15. Peña-Gallego A, Hernández-Orte P, Cacho J, Ferreira V. High-Performance Liquid Chromatography
421 Analysis of Amines in Must and Wine: A Review. *Food Reviews International*. 2012;28(1):71-96.
- 422 16. García-Villar N, Hernández-Cassou S, Saurina J. Determination of biogenic amines in wines by pre-
423 column derivatization and high-performance liquid chromatography coupled to mass spectrometry.
424 *Journal of Chromatography A*. 2009;1216(36):6387-93.
- 425 17. Cunha SC, Faria MA, Fernandes JO. Gas Chromatography–Mass Spectrometry Assessment of
426 Amines in Port Wine and Grape Juice after Fast Chloroformate Extraction/Derivatization. *Journal of*
427 *Agricultural and Food Chemistry*. 2011;59(16):8742-53.
- 428 18. Daniel D, Santos V, Tadeu Rajh Vidal D, do Lago C. Determination of biogenic amines in beer and
429 wine by capillary electrophoresis-tandem mass spectrometry2015.
- 430 19. Kivirand K, Rinken T. Biosensors for Biogenic Amines: The Present State of Art Mini-Review.
431 *Analytical Letters*. 2011;44(17):2821-33.
- 432 20. Basozabal I, Guerreiro A, Gomez-Caballero A, Aranzazu Goicolea M, Barrio RJ. Direct
433 potentiometric quantification of histamine using solid-phase imprinted nanoparticles as recognition
434 elements. *Biosensors and Bioelectronics*. 2014;58:138-44.
- 435 21. Henao-Escobar W, del Torno-de Román L, Domínguez-Renedo O, Alonso-Lomillo MA, Arcos-
436 Martínez MJ. Dual enzymatic biosensor for simultaneous amperometric determination of histamine and
437 putrescine. *Food Chemistry*. 2016;190:818-23.

- 438 22. Marcobal A, Polo MC, Martín-Álvarez PJ, Moreno-Arribas MV. Biogenic amine content of red
439 Spanish wines: comparison of a direct ELISA and an HPLC method for the determination of histamine in
440 wines. *Food Research International*. 2005;38(4):387-94.
- 441 23. Hernández-Cassou S, Saurina J. Determination of Histamine in Wine Samples by Flow-Injection
442 Analysis and Multivariate Calibration. *Analytical Letters*. 2013;46(11):1758-68.
- 443 24. T. Surya BS, V. Alamelu, A. Priyatharshini, U. Arisekar and S. Sundhar. Rapid Methods for
444 Histamine Detection in Fishery Products. *International Journal of Current Microbiology and Applied
445 Sciences* 2019;8.
- 446 25. Mak WC, Beni V, Turner APF. Lateral-flow technology: From visual to instrumental. *TrAC Trends
447 in Analytical Chemistry*. 2016;79:297-305.
- 448 26. Wang D-B, Tian B, Zhang Z-P, Deng J-Y, Cui Z-Q, Yang R-F, et al. Rapid detection of *Bacillus
449 anthracis* spores using a super-paramagnetic lateral-flow immunological detectionsystem. *Biosensors and
450 Bioelectronics*. 2013;42:661-7.
- 451 27. Wang D-B, Tian B, Zhang Z-P, Wang X-Y, Fleming J, Bi L-J, et al. Detection of *Bacillus anthracis*
452 spores by super-paramagnetic lateral-flow immunoassays based on “Road Closure”. *Biosensors and
453 Bioelectronics*. 2015;67:608-14.
- 454 28. Wang Y, Xu H, Wei M, Gu H, Xu Q, Zhu W. Study of superparamagnetic nanoparticles as labels in
455 the quantitative lateral flow immunoassay. *Materials Science and Engineering: C*. 2009;29(3):714-8.
- 456 29. Zheng C, Wang X, Lu Y, Liu Y. Rapid detection of fish major allergen parvalbumin using
457 superparamagnetic nanoparticle-based lateral flow immunoassay. *Food Control*. 2012;26(2):446-52.
- 458 30. Lago-Cachón D, Rivas M, Martínez-García JC, García JA. Cu impedance-based detection of
459 superparamagnetic nanoparticles. *Nanotechnology*. 2013;24(24):245501.
- 460 31. Rivas M, Lago-Cachón D, Martínez-García JC, García JA, Calleja AJ. Eddy-current sensing of
461 superparamagnetic nanoparticles with spiral-like copper circuits. *Sensors and Actuators A: Physical*.
462 2014;216:123-7.
- 463 32. Lago-Cachón D, Oliveira-Rodríguez M, Rivas M, Blanco-López MC, Martínez-García JC, Moyano
464 A, et al. Scanning Magneto-Inductive Sensor for Quantitative Assay of Prostate-Specific Antigen. *IEEE
465 Magnetics Letters*. 2017;8:1-5.
- 466 33. Bica D, Vékás L, Avdeev MV, Marinică O, Socoliuc V, Bălăsoiu M, et al. Sterically stabilized water
467 based magnetic fluids: Synthesis, structure and properties. *Journal of Magnetism and Magnetic Materials*.
468 2007;311(1):17-21.
- 469 34. Redruello B, Ladero V, del Rio B, Fernández M, Martín M, Alvarez M. A UHPLC method for the
470 simultaneous analysis of biogenic amines, amino acids and ammonium ions in beer. *Food Chemistry*.
471 2016;217:117-24.
- 472 35. Rodbard D. Statistical Quality Control and Routine Data Processing for Radioimmunoassays and
473 Immunoradiometric Assays. *Clinical Chemistry*. 1974;20(10):1255.
- 474 36. Aguilar-Arteaga K, Rodriguez JA, Barrado E. Magnetic solids in analytical chemistry: A review.
475 *Analytica Chimica Acta*. 2010;674(2):157-65.
- 476 37. Hayashi Y, Matsuda R, Maitani T, Imai K, Nishimura W, Ito K, et al. Precision, Limit of Detection
477 and Range of Quantitation in Competitive ELISA. *Analytical chemistry*. 2004;76(5):1295-301.
- 478

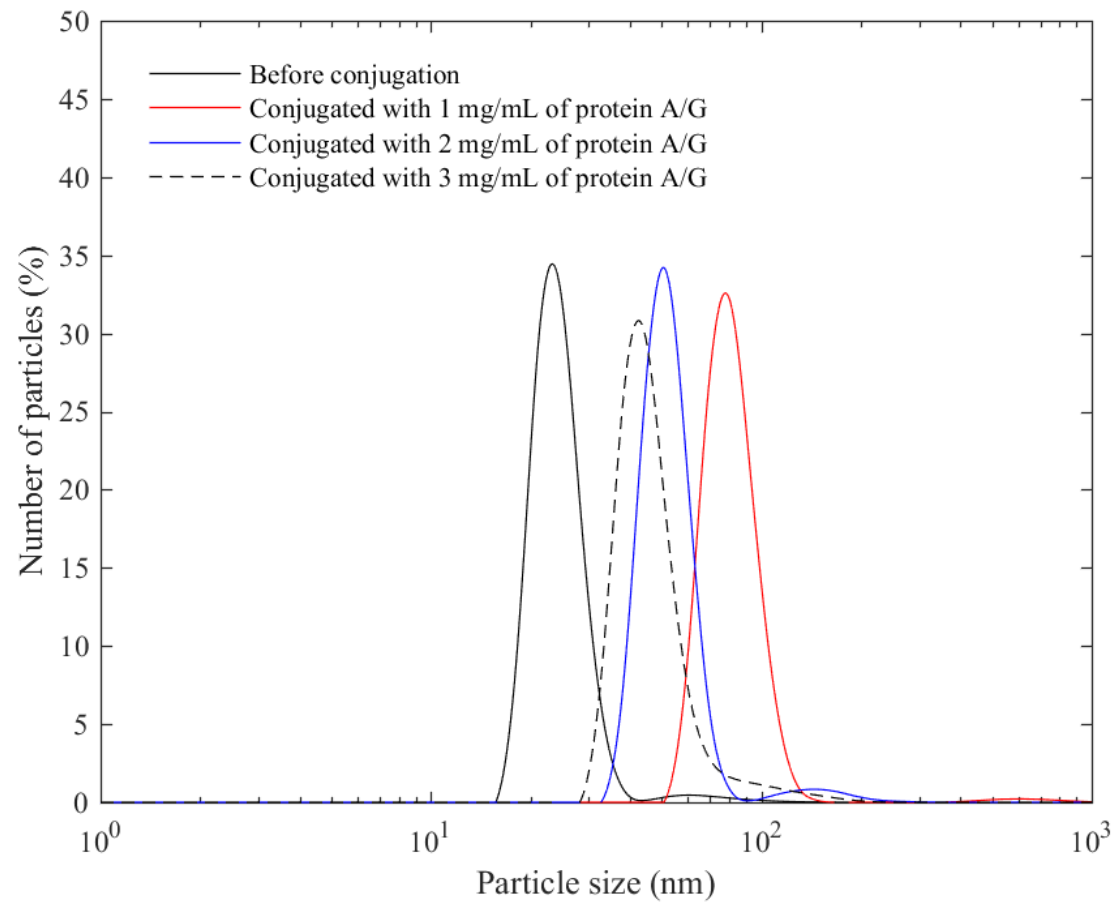
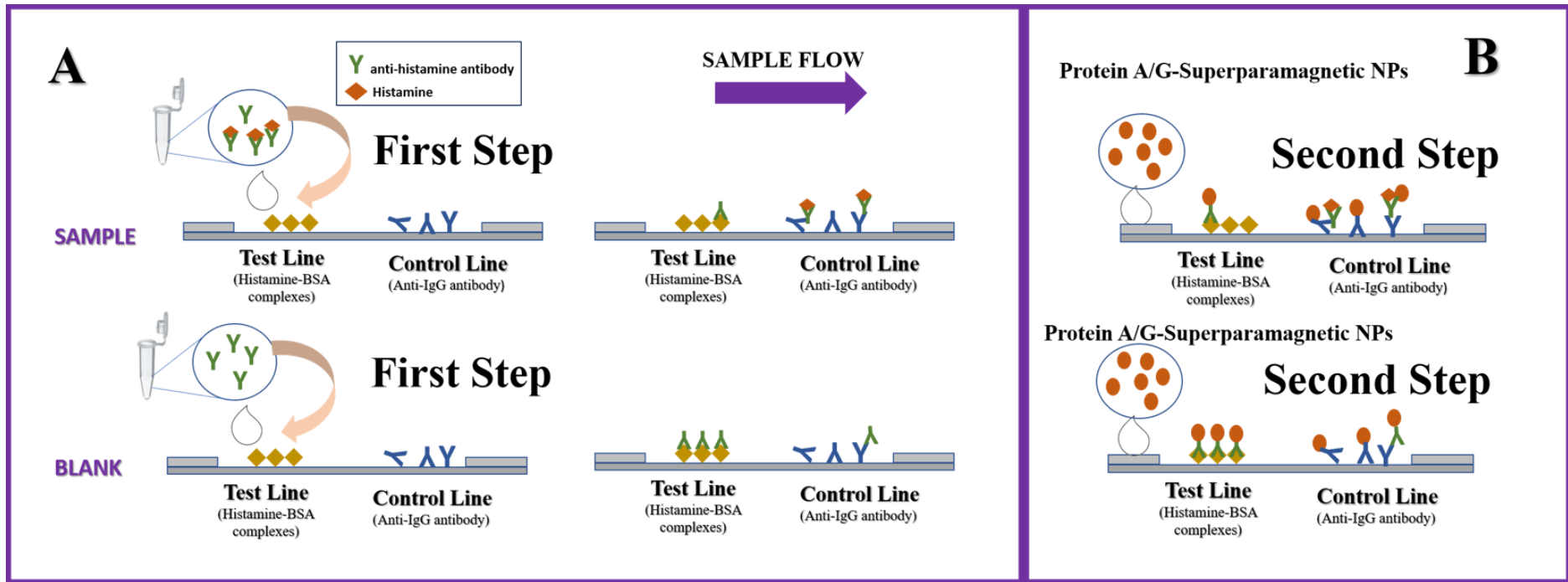


Figure 1. Hydrodynamic size distribution profiles of superparamagnetic iron oxide nanoparticles before (solid black line) and after conjugation with concentrations of 1 mg/mL (red), 2 mg/mL (blue) and 3 mg/mL (dashed) of protein A/G.



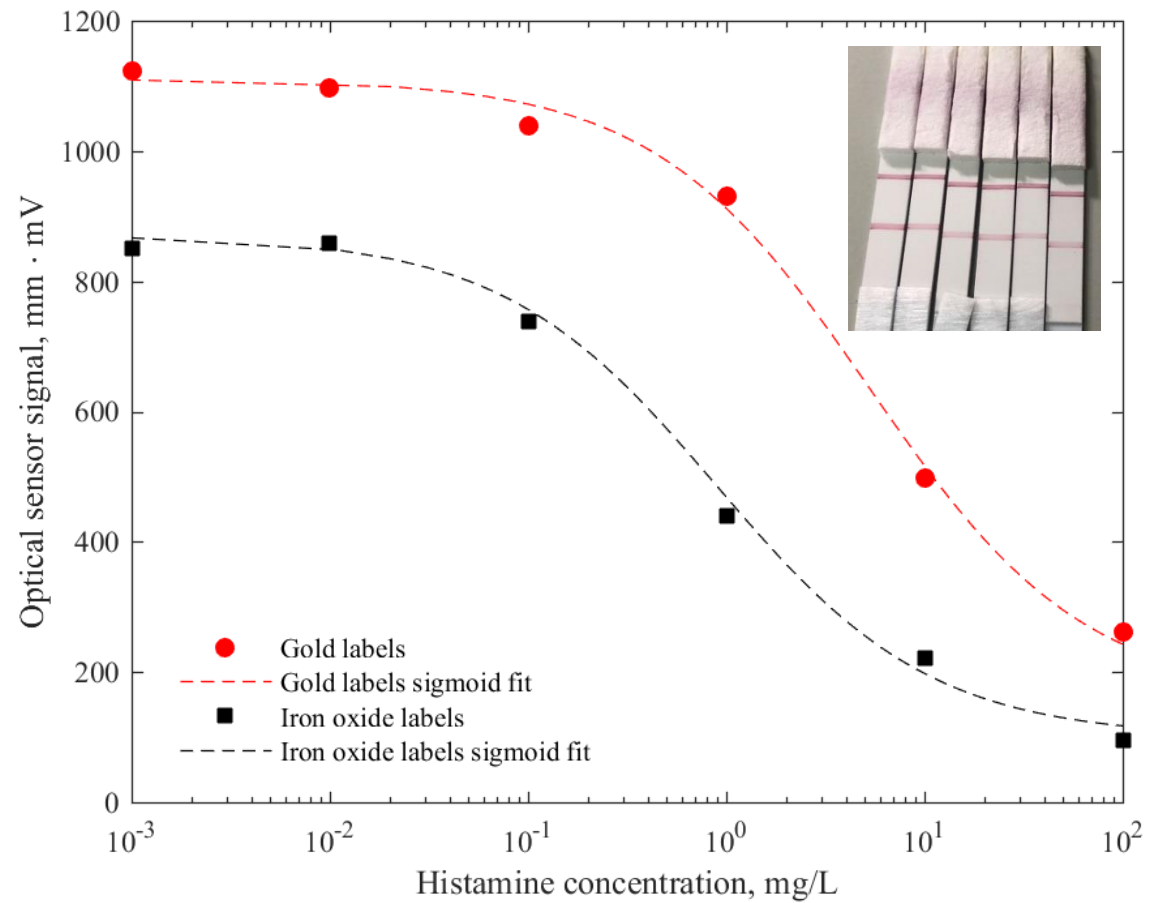


Figure 3. Quantification of LFIAs by the optical reader using gold (red) and iron oxide (black) NPs. The lines plotted to guide the eye are four-parameter sigmoid curves. Inset: One of the series of standard samples used to obtain the red curve, with the control line on top and the test line below.

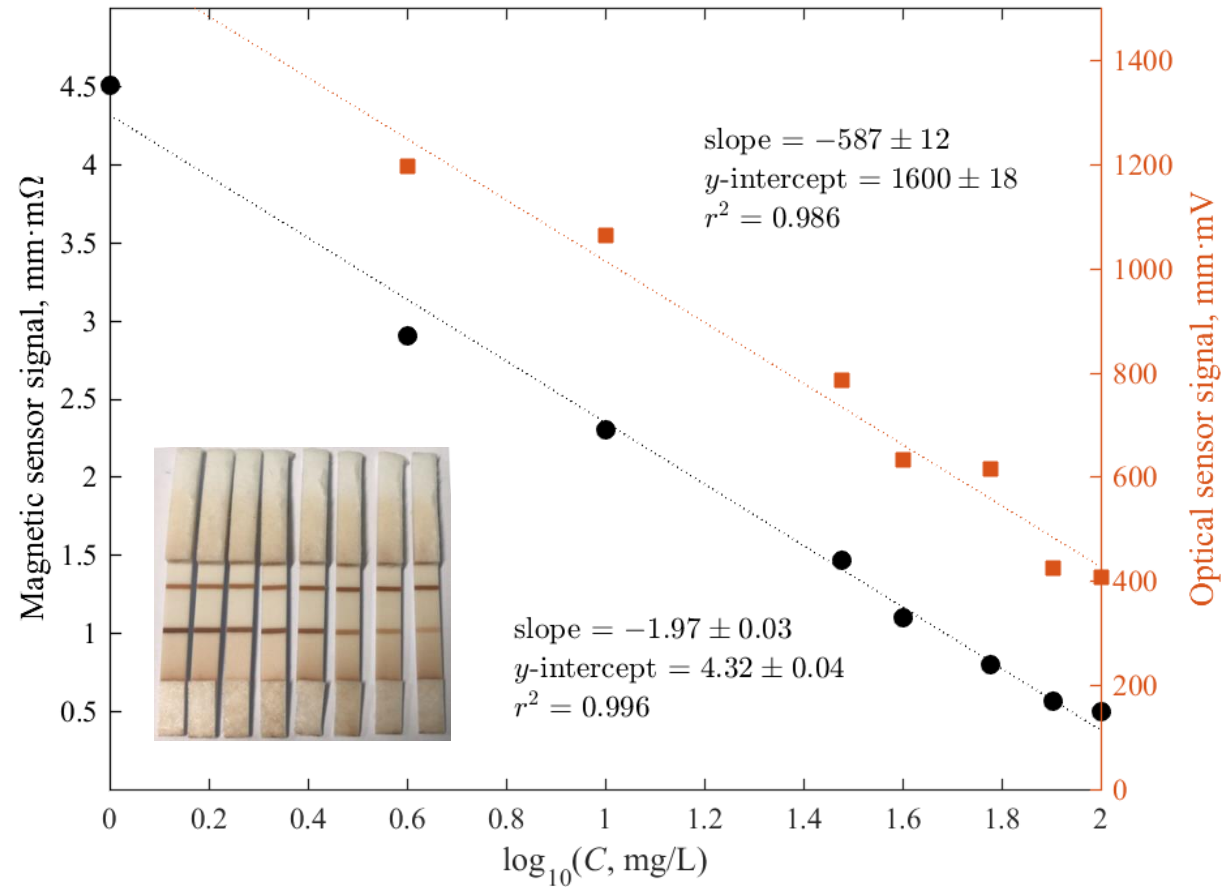


Figure 4. Inductive (left axis) and optical (right axis) signals of the magnetic LFIA as a function of the concentration of histamine. Least-squares linear regression curves are plotted as dotted lines. Inset: One of the series of standard samples used to obtain the plotted lines. The control line is on top and the test line below.



Figure 5. LFIs run with red wine samples using (A) superparamagnetic nanoparticles and (B) colloidal gold as reporters.